

# Modeling the adsorption of mercury in the flue gas of sewage sludge incineration

Oliver Malerius<sup>1</sup>, Joachim Werther\*

Chemical Engineering I, Technical University Hamburg at Harburg, D-21071 Hamburg, Germany

## Abstract

Today, mercury is regarded as one of the most harmful substances for the environment. Therefore, legislation is setting increasingly strict flue gas emission limits. Since not in all existing incineration plants special concepts of mercury removal have been foreseen, problems to meet new low emission limit values may rise. Adsorbent injection is one way to reduce the mercury concentration of the flue gas which can in existing plants be installed upstream of the particle removal device. This paper presents a model for the mercury removal in the dust laden flue gas upstream of an electrostatic precipitator. After the investigation of different adsorbents in a laboratory test facility, the adsorption parameters are calculated and the model is used to show the influence of the governing parameters on the adsorption process and to simulate the efficiency of mercury capture in an existing sewage sludge incineration plant. The mercury removal with the fly ash as an adsorbent is simulated and compared with measurements obtained in an industrial plant.

© 2003 Elsevier B.V. All rights reserved.

*Keywords:* Flue gas; Adsorption; Mercury

## 1. Introduction

Mono-combustion of sewage sludge is practiced predominantly in fluidized bed combustors. The 17th BImSchV (i.e. the 17th regulation for the federal emission law) is applicable for waste incineration in Germany. It is setting an average daily emission limit of  $30 \mu\text{g mercury}/\text{m}^3$  flue gas (under standard conditions, dry basis, referred to 11 vol.% oxygen in the flue gas). The observance of this very restrictive mercury emission limit in flue gas is not possible without special abatement facilities. In modern sewage sludge incineration plants the meeting of this threshold limit is safely achieved by special mercury removal concepts in scrubbers or entrained flow adsorbers (e.g. [5,8]).

Problems may rise in older plants without highly sophisticated mercury removal facilities. In these cases peaks of mercury in the fuel or an increase in the mercury input may lead to mercury concentrations in the clean gas above the limit and with that cause problems in the continuous operation of the plant. In these plants either the mercury removal has to be generally enhanced or mercury peaks have to be caught

by discontinuously operating mercury removal devices. The adsorption of mercury is one way to enhance the overall mercury removal in existing plants. In practice different adsorbers are operated to remove the mercury: namely fixed beds, moving beds, circulating fluidized beds or entrained flow adsorbers. The adsorption is influenced by different parameters, e.g. flue gas temperature, Hg concentration and adsorbent properties. The adsorption principle could be applied to existing plants if the adsorbent could be injected upstream of the existing dust removal unit.

The present work is part of efforts to improve the mercury capture at the sewage sludge incineration plant operated by InfraServ GmbH & Co. Höchst KG at its site in Frankfurt, Germany. A flow sheet of this incineration plant is shown in Fig. 1. Industrial and municipal sewage sludge is incinerated here with an annual throughput of 130,000 t dry matter in two parallel lines. The incineration takes place in stationary fluidized beds. The flue gas is after heat recovery cleaned in an electrostatic precipitator (ESP) followed by a venturi scrubber and a radial flow scrubber. The main mercury sink is the venturi scrubber which, however, extracts only mercury in its ionic form. In order to capture also elemental mercury and increase the overall efficiency of the mercury capture a work program for the investigation of possibilities of adsorption with sorbent injection upstream of the ESP was initiated. In the following a model of adsorption in the entrained flow will be described.

*Abbreviations:* d.b., dry basis; s.c., standard conditions (1 bar, 273 K)

\* Corresponding author. Tel.: +49-40-42878-3039;  
fax: +49-40-42878-2678.

*E-mail address:* werther@tu-harburg.de (J. Werther).

<sup>1</sup> Present address: Lurgi Energie und Entsorgung GmbH, D-40880 Ratingen, Germany.

### Nomenclature

$a$	mass specific surface area ( $\text{m}^2/\text{kg}$ )
$A_t$	cross-sectional area of duct ( $\text{m}^2$ )
$c$	concentration ( $\text{kg}/\text{m}^3$ )
$k$	constant defined by Eq. (12) (–)
$k_{\text{ads}}$	adsorption constant in Eq. (15) ( $\text{kg}/(\text{m}^2 \text{ s})$ )
$K$	constant defined by Eq. (13) (–)
$M$	mass (kg)
$\dot{M}$	mass flow ( $\text{kg}/\text{s}$ )
$n$	parameter, defined by Eq. (12) (–)
$R$	adsorption rate based on unit adsorber volume ( $\text{kg}/(\text{s m}^3)$ )
$\hat{R}$	adsorption rate ( $\text{kg}/\text{s}$ )
$S^2$	parameter defined by Eq. (14) (–)
$S_x^2$	variance of $x$ (–)
$S_y^2$	variance of $y$ (–)
$S_{xy}^2$	covariance of $x$ and $y$ (–)
$t$	time (s)
$u$	superficial gas velocity (m/s)
$X$	Hg concentration on the solid phase ( $\text{kg}/\text{kg}$ )
$X_{\text{eq}}$	equilibrium concentration defined by Eq. (15) (–)
$X_{\text{max}}$	concentration defined by Eq. (13) (–)
$Y$	Hg concentration in the gas phase ( $\text{kg}/\text{kg}$ )
$Y'$	Hg concentration in the gas phase ( $\text{kg}/\text{m}^3$ )
$z$	coordinate along the flue gas path (m)
<i>Greek symbols</i>	
$\mu$	solids loading of the gas flow ( $\text{kg}/\text{kg}$ )
$\rho$	density ( $\text{kg}/\text{m}^3$ )

## 2. Model development

The injection of an adsorbent upstream of the dust removal device is one option to reduce the mercury content in the flue gas of existing sewage sludge incineration plants. In order to assess the feasibility of such a concept it would be

helpful to forecast the mercury removal efficiency by model calculations.

Based on the assumption that Hg is adsorbed in a very dilute suspension of adsorbent particles in the flue gas and that the velocity of the adsorbent particles is roughly equal to the flue gas velocity the mass balance of mercury in the gas phase and on the solid phase can be derived. Fig. 2 shows a volume element  $\Delta z A_t$  of the flue gas duct. The mass balance of mercury in the flue gas is then

$$\frac{dM_{\text{Hg,gas}}}{dt} = \dot{M}_{\text{Hg,gas,in}} - \dot{M}_{\text{Hg,gas,out}} - \hat{R} \quad (1)$$

$\hat{R}$  describes the mass that is removed per unit time from the gas phase by adsorption on the adsorbent particle surface. The input mass flow of mercury is

$$\dot{M}_{\text{Hg,gas,in}} = \dot{M}_{\text{gas}} Y_{\text{Hg}} = \rho_{\text{gas}} u A_t Y_{\text{Hg}} \quad (2)$$

For the mass flow of mercury in the flue gas that leaves the volume element it holds

$$\begin{aligned} \dot{M}_{\text{Hg,gas,out}} &= \dot{M}_{\text{Hg,in}} + \frac{\partial \dot{M}_{\text{Hg,in}}}{\partial z} dz \\ &= \dot{M}_{\text{gas}} Y_{\text{Hg}} + \dot{M}_{\text{gas}} \frac{\partial Y_{\text{Hg}}}{\partial z} dz, \\ \dot{M}_{\text{Hg,gas,out}} &= \rho_{\text{gas}} u A_t Y_{\text{Hg}} + \rho_{\text{gas}} u A_t \frac{\partial Y_{\text{Hg}}}{\partial z} dz \end{aligned} \quad (3)$$

Assuming a stationary case, it follows:

$$\rho_{\text{gas}} u \frac{dY_{\text{Hg}}}{dz} = -R \quad (4)$$

where  $R$  denotes the Hg adsorption rate based on unit volume of the flue gas duct,

$$R = \frac{\hat{R}}{V} \quad (5)$$

and the Hg concentration in the flue gas is given by

$$Y_{\text{Hg}} = \frac{M_{\text{Hg}}}{M_{\text{Gas}}} \quad (6)$$

With the same assumptions similar equations for the Hg loading on the adsorbent can be developed. The

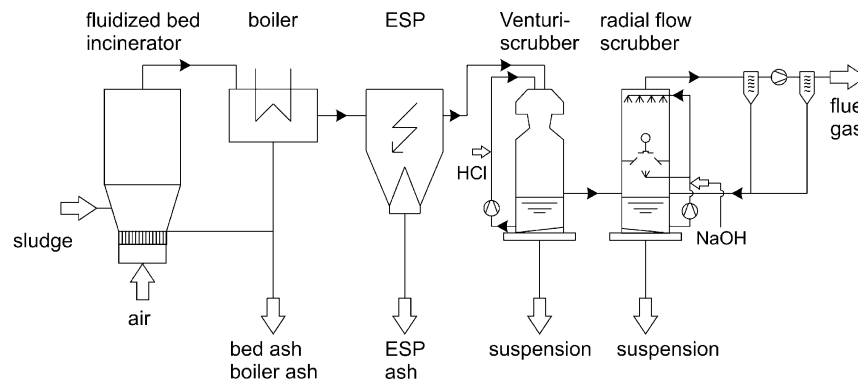


Fig. 1. Flow sheet of the sewage sludge incineration plant operated by InfraServ GmbH & Co. Höchst KG at its site in Frankfurt, Germany.

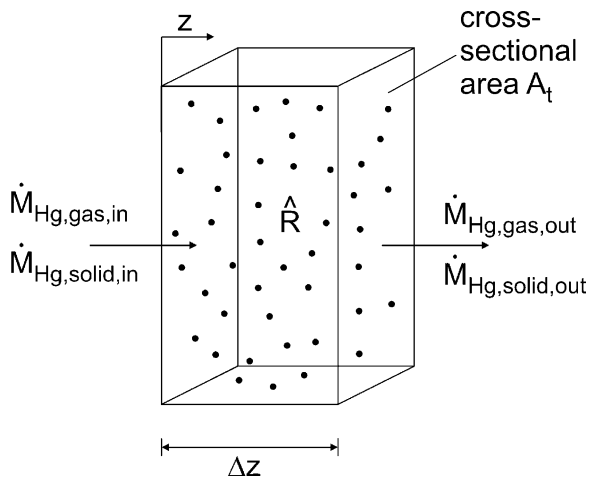


Fig. 2. Schematic picture of a volume element of the flue gas channel upstream of the particle removal device.

time-dependent change of the Hg mass, the Hg input and output are described as follows:

$$\frac{dM_{\text{Hg,solid}}}{dt} = \dot{M}_{\text{Hg,in}} - \dot{M}_{\text{Hg,out}} + \hat{R} \quad (7)$$

$$\dot{M}_{\text{Hg,in}} = \dot{M}_{\text{solid}} X_{\text{Hg}} = \mu \rho_{\text{gas}} u A_t X_{\text{Hg}} \quad (8)$$

$$\begin{aligned} \dot{M}_{\text{Hg,out}} &= \dot{M}_{\text{solid}} X_{\text{Hg}} + \dot{M}_{\text{solid}} \frac{\partial X_{\text{Hg}}}{\partial z} dz \\ &= \mu \rho_{\text{gas}} u A_t X_{\text{Hg}} + \mu \rho_{\text{gas}} u A_t \frac{\partial X_{\text{Hg}}}{\partial z} dz \end{aligned} \quad (9)$$

where  $\mu$  is the solids loading of the flue gas in kg adsorbent/kg flue gas.

Under stationary conditions it holds

$$\mu \rho_{\text{gas}} u \frac{dX_{\text{Hg}}}{dz} = R \quad (10)$$

with the Hg loading on the sorbent

$$X_{\text{Hg}} = \frac{M_{\text{Hg}}}{M_{\text{solid}}} = \frac{1}{\mu} \frac{M_{\text{Hg}}}{M_{\text{gas}}} \rho_{\text{gas}} \quad (11)$$

Assuming that the process is not limited by mass transfer and if the adsorption parameters are known the balance equations can be solved with the following start conditions:

1. the mercury content on the solid is zero at  $z = 0$  (i.e. at the point of injection);
2. the mercury concentration of the flue gas at  $z = 0$  equal to the Hg concentration at the output of the boiler.

The differential equations are solved using Mathcad Professional 7 (Mathsoft) with a Runge–Kutta process (function rkadapt()).

### 3. Determination of the adsorption parameters

In a laboratory-scale test rig the adsorption parameters were evaluated by measuring breakthrough curves in the following way: nitrogen was loaded with a certain concentration of mercury. The gas flowed then through a fixed bed of the investigated adsorbent. The mercury concentration downstream of the fixed bed was measured continuously until 95% of the input concentration was reached (breakthrough).

Fig. 3 shows a schematic drawing of the experimental set-up. The mercury concentration was adjusted by the controlled addition of a mercury standard solution (mercury-spectroscopy standard ( $\text{Hg}(\text{NO}_3)_2 \cdot \text{H}_2\text{O}$ , 1 g/l)) into a reducing solution of tin chloride ( $c = 50$  g/l). By variation of the dosage the Hg concentration in the gas was adjusted. The gas was heated up to the adsorption temperature using a temperature controlled heating hose and passes the thermostatic fixed bed. The adsorbent mass was varied between 0.5 and 3 g depending on the different adsorbent capacities. The adsorbent was mixed with 5 g of inert material (quartz sand) to achieve a longer adsorption zone. Downstream of the adsorption system the mercury concentration was measured using a continuous mercury analyzer (Seefeldler Hg-Monitor 2000 with chemical pretreatment, Seefeldler Meßtechnik, Germany). The measured breakthrough curve was used to calculate the equilibrium data.

Breakthrough curves were measured for different Hg concentrations between  $50 \mu\text{g}/\text{m}^3$  (d.b., s.c.) and  $1200 \mu\text{g}/\text{m}^3$  (d.b., s.c.) and different gas temperatures (60, 120 and  $180^\circ\text{C}$ ). Adsorbents based on activated carbon were used only up to  $120^\circ\text{C}$  to avoid the risk of hot-spot formation. The calculated equilibrium concentrations were verified by analysis of the adsorbent samples in the central chemical laboratory of the university. Table 1 shows the adsorbents investigated and their characteristics.

It should be noted that due to the production of mercury by reduction in a gas wash bottle a water content of 5 vol.% was found in the gas. This water content can influence the

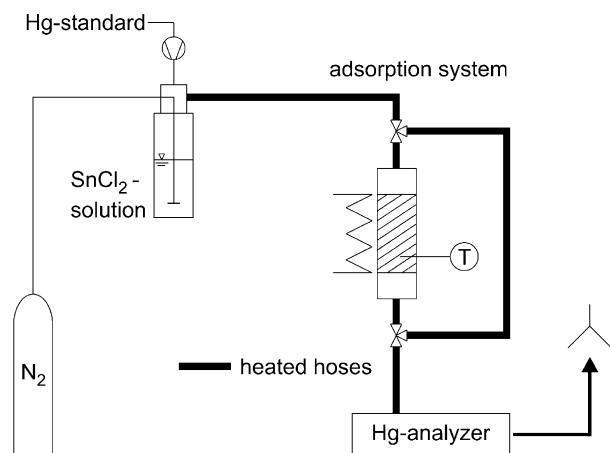


Fig. 3. Laboratory set-up for adsorption tests.

Table 1  
Characterization of the adsorbents<sup>a</sup>

Adsorbent	Bulk density (kg/m <sup>3</sup> )	Specific surface area (m <sup>2</sup> /g)	S content (mass%)	d <sub>50.3</sub> (μm)
Activated carbon	590	800 <sup>b</sup>	–	25
S-impregnated activated carbon	530	1000 <sup>b</sup>	10	25
S-impregnated zeolite	750	79 <sup>b</sup>	n.d.	25
Fly ash (TUHH)	1650	0.17 <sup>c</sup>	n.d.	130
Fly ash (Höchst)	2060	0.356 <sup>c</sup>	n.d.	32
Fly ash (VERA)	1890	0.26 <sup>c</sup>	n.d.	70

<sup>a</sup> d<sub>50.3</sub> is the 50% value of the cumulative mass distribution of particle sizes measured by laser diffraction analysis, fly ash (TUHH) the ash generated in the university's pilot-scale incineration facility, fly ash (Höchst) is from the InfraServ incinerator and fly ash (VERA) is from the city of Hamburg's sewage sludge incineration plant; n.d.: not determined.

<sup>b</sup> BET surface area

<sup>c</sup> Specific surface area calculated using particle size distribution.

Table 2  
Adsorption equilibrium data (Langmuir type)

	60 °C			120/180 °C		
	K (–)	X <sub>max</sub> (kg/kg)	S <sup>2</sup> (–)	K (–)	X <sub>max</sub> (kg/kg)	S <sup>2</sup> (–)
Activated carbon	2.99E6	1.41E–3	0.89	2.49E6	8.09E–4	0.92
Ash (TUHH)	8.7E6	1.91E–5	0.9	8.7E6	2.11E–5	0.89
Ash (Höchst)	–	–	–	7.23E6	1.75E–5	0.9
Ash (VERA, Hamburg)	–	–	–	6.48E6	5.49E–6	0.88

adsorption process. In real flue gases of sewage sludge combustions the water content of the flue gas can be up to 30 vol. %.

In this work two adsorption theories, that were also applied by Meserole et al. [6] and Serre and Silcox [7] are used to describe the data obtained during the laboratory-scale tests, i.e., the adsorption theory according to Freundlich:

$$X = kY^n \quad (12)$$

where the adsorption parameters  $k$  and  $n$  are calculated with the use of the equilibrium data of the breakthrough curves and in addition the adsorption theory according to Langmuir. The Langmuir relationship

$$X = \frac{KX_{\max}Y}{1 + KY} \quad (13)$$

is valid for mono-molecular connection of the adsorptive on the adsorbent surface. The parameters  $K$  and  $X_{\max}$ , in the above equation have to be determined from the experiments.

The parameters in Eqs. (12) and (13) were calculated by non-linear regression of the equilibrium data. The quality of

the regression was judged by calculating the parameter  $S^2$ ,

$$S^2 = \frac{S_{xy}^2}{S_x^2 S_y^2} \quad (14)$$

which is calculated as the covariance divided by the variances of the data. At  $S^2 = 1$  the regression curve is fitting all data points [1].

During the calculations it was found that the equilibrium data of the ashes and activated carbon (Table 2) were best fitted with the Langmuir relationship, whereas the data of S-impregnated zeolite and S-impregnated activated carbon (Table 3) are better fitted by the Freundlich theory. Fig. 4 gives four examples. Since the value of  $S^2$  is in most cases around 0.9, the data are fitted sufficiently well.

The kinetic parameters of the adsorption process were also calculated from the experimentally determined breakthrough curves. It is assumed that the adsorption process is not limited by mass transfer [7]. The following modified adsorption kinetics are used for the correlation of the data [3]:

$$R = k_{\text{ads}} Y \mu a (X_{\text{eq}} - X) \quad (15)$$

Table 3  
Adsorption equilibrium data (Freundlich type)

	60 °C			120/180 °C		
	K (–)	n (–)	S <sup>2</sup> (–)	K (–)	n (–)	S <sup>2</sup> (–)
S-activated carbon	5.58E7	1.687	0.89	5.08E7	1.703	0.94
S-zeolite	1.01E7	1.793	0.91	1.2E7 (180 °C)	1.819 (180 °C)	0.9 (180 °C)
				1.35E7 (120 °C)	1.801 (120 °C)	0.98 (120 °C)

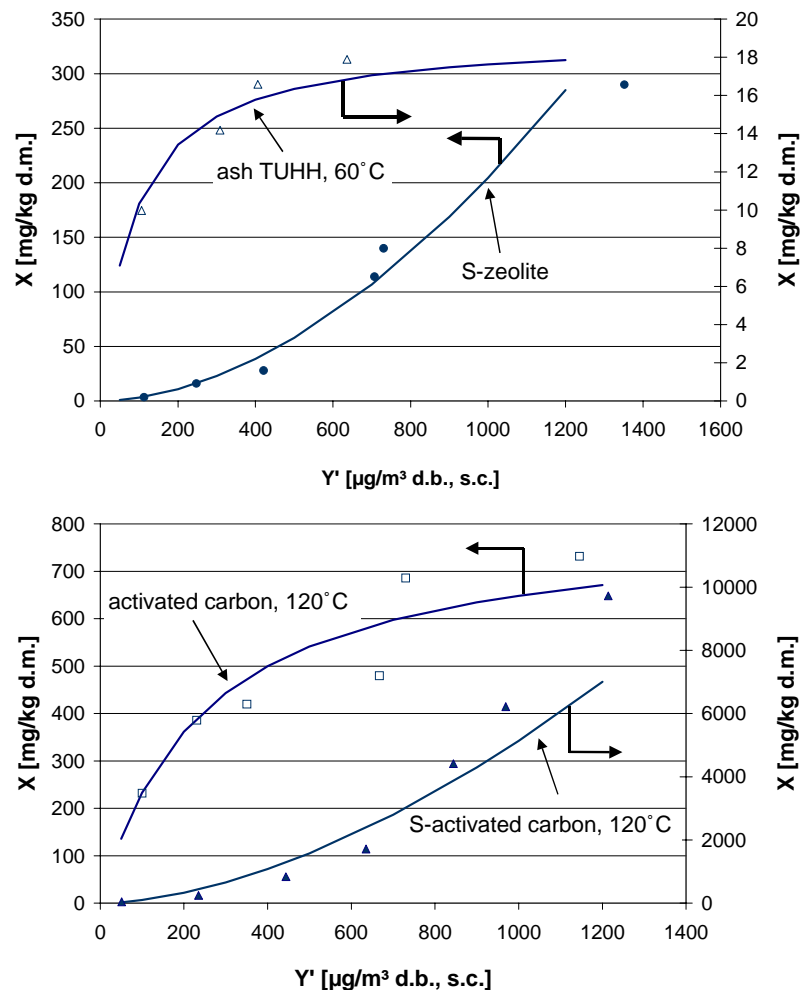


Fig. 4. Examples of measured adsorption isotherms. The Langmuir-type isotherm was used to fit ash TUHH ( $K = 8.7E6$ ,  $X_{\max} = 19 \text{ mg/kg}$ ,  $S^2 = 0.9$ ) and the activated Carbon ( $K = 2.49E6$ ,  $X_{\max} = 809 \text{ mg/kg}$ ,  $S^2 = 0.9$ ). The S-zeolite ( $K = 1.35E7$ ,  $n = 1.80$ ,  $S^2 = 0.98$ ) and the S-activated Carbon ( $K = 5.08E7$ ,  $n = 1.703$ ,  $S^2 = 0.94$ ) were fitted with a Freundlich-type isotherm.

where  $X_{\text{eq}}$  denotes the equilibrium Hg concentration on the adsorbent and  $a$  the mass specific surface area of the adsorbent. For the determination of the kinetic parameter  $k_{\text{ads}}$  the breakthrough curves were fitted basically with the model described above. The model was used to calculate the concentration downstream of the fixed bed, which was then used as the new input concentration. The curve was fitted by adjusting the kinetic parameter. Table 4 shows the values of  $k_{\text{ads}}$  for the investigated adsorbents.

Table 4  
Kinetic parameters at 120 °C for adsorbents based on activated carbon and at 180 °C for zeolite and ash

Adsorbent	Kinetic parameter, $k_{\text{ads}}$ (kg/(m <sup>2</sup> s))
Activated carbon	$8.5 \times 10^{-3}$
S-impregnated activated carbon	$5.5 \times 10^{-2}$
S-zeolite	32.5
Ash (TUHH)	10450
Ash (Höchst)	8350
Ash (VERA, Hamburg)	6750

## 4. Results and discussion

### 4.1. Influence of different parameters on the adsorption process

Based on the models described above the influence of the various parameters on the adsorption process can be investigated. The most significant parameters are the mercury concentration in the flue gas, the flue gas residence time, the adsorbent capacity, the adsorbent mass and the specific surface area of the adsorbent.

The operation data and the flue gas duct dimensions of the sewage sludge combustion operated by InfraServ Höchst are the basis for the parameter variation. An overview of the data is given in Table 5. The adsorbent is assumed to be added immediately after the boiler. The influence of the residence time is shown in all the following figures, because the Hg concentration in the flue gas and on the adsorbent are always shown depending on the length of the flue gas duct. With a flue gas velocity of 7.9 m/s the residence time in the

Table 5  
Parameters of the Höchst incineration plant

Volumetric flue gas flow ((m <sup>3</sup> d.b., s.c.)/h)	25300
$T$ (flue gas after heat recovery boiler) (°C)	220
Ash concentration in the flue gas (g/m <sup>3</sup> )	24
Cross-sectional area of flue gas duct (m <sup>2</sup> )	1.58
Length of flue gas duct between boiler and ESP (m)	23.6
Residence time of flue gas between heat recovery boiler and ESP (s)	3
Residence time of the flue gas in the ESP (s)	12

flue gas duct between the boiler and the ESP is roughly 3 s. Note that the residence time of the flue gas in the ESP is very high due to its huge volume.

Figs. 5–8 show that in all cases with increasing residence time the adsorption process advances which results in lower flue gas and higher adsorbent Hg concentrations with increasing length of the flue gas duct. At first Fig. 5 shows the influence of the input Hg flue gas concentration on the adsorption of Hg on the adsorbent particles. The upper diagram presents the changes in the flue gas concentration and the lower diagram in the Hg concentration on the adsorbent. With increasing mercury concentration in the input flue gas the Hg concentration on the adsorbent at the end of the flue gas duct increases. At a flue gas concentration of 1000  $\mu\text{g Hg/m}^3$  (d.b., s.c.) the adsorbent leaving the flue gas duct is loaded with 240 mg Hg/kg d.m. at a total capacity of 250 mg/kg d.m. Simultaneously  $c/c_0$  is decreased to 0.7

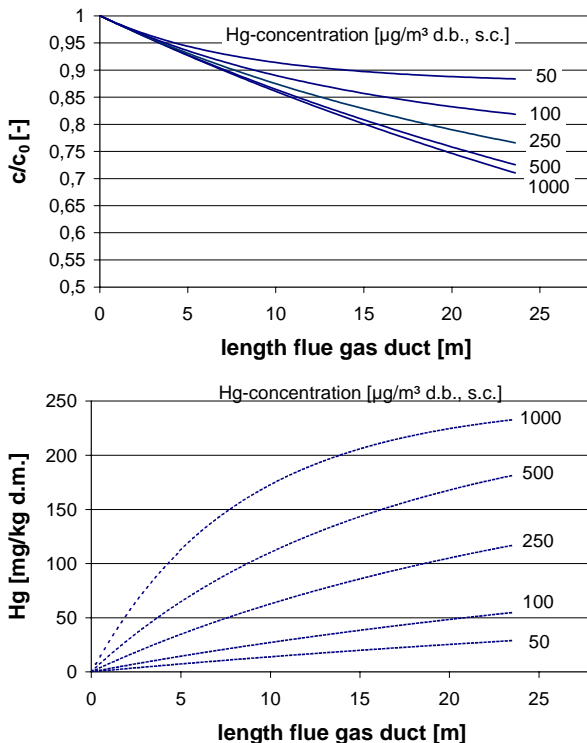


Fig. 5. Influence of the input concentration of Hg in the flue gas on the adsorption of Hg on the adsorbent:  $k_{\text{ads}} = 1 \text{ kg}/(\text{m}^2 \text{ s})$ ,  $X_{\text{eq}} = 250 \text{ mg}/\text{kg}$ , specific surface area  $a = 500 \text{ m}^2/\text{g}$ , mass concentration of the adsorbent in the flue gas is  $0.5 \text{ g}/\text{m}^3$  (d.b., s.c.).

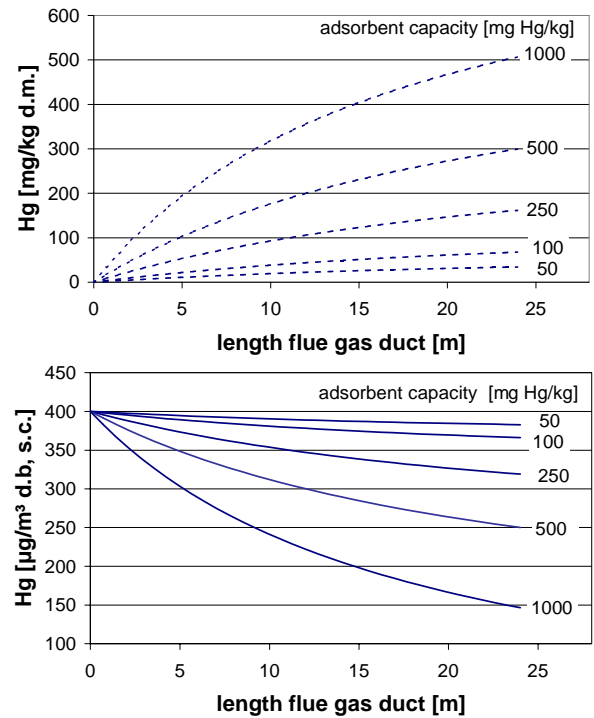


Fig. 6. Influence of the adsorbent capacity on the Hg adsorption:  $k_{\text{ads}} = 1 \text{ kg}/(\text{m}^2 \text{ s})$ ,  $a = 500 \text{ m}^2/\text{g}$ , mass concentration of the adsorbent in the flue gas is  $0.5 \text{ g}/\text{m}^3$  (d.b., s.c.), input Hg concentration  $400 \text{ mg}/\text{m}^3$  (d.b., s.c.).

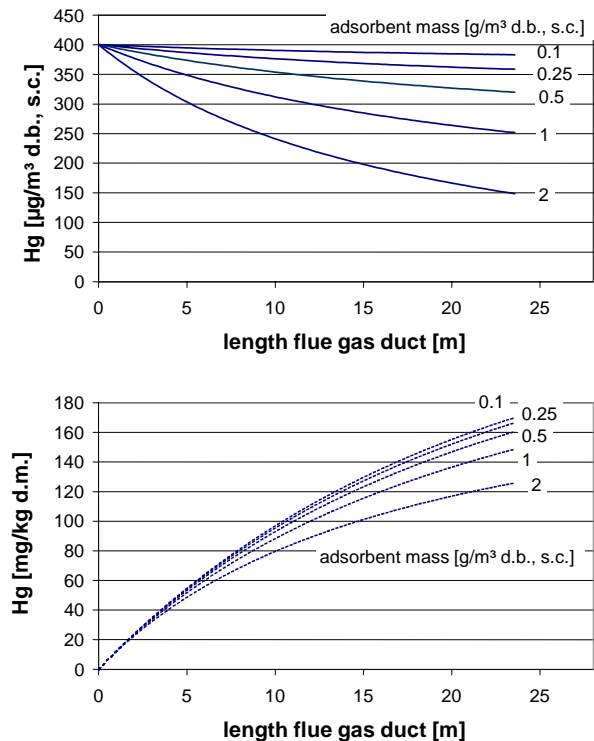


Fig. 7. Influence of the mass concentration of the adsorbent on Hg adsorption:  $k_{\text{ads}} = 1 \text{ kg}/(\text{m}^2 \text{ s})$ ,  $X_{\text{eq}} = 250 \text{ mg}/\text{kg}$ ,  $a = 500 \text{ m}^2/\text{g}$ ,  $C_0 = 400 \text{ mg}/\text{m}^3$  (d.b., s.c.).

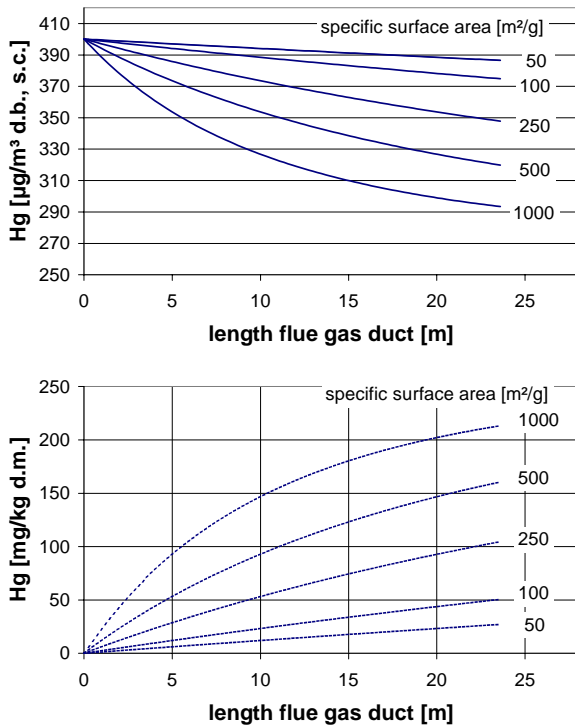


Fig. 8. Influence of the specific surface area of the adsorbent on the Hg adsorption on the particles:  $k_{\text{ads}} = 1 \text{ kg}/(\text{m}^2 \text{ s})$ ,  $X_{\text{eq}} = 250 \text{ mg}/\text{kg}$ , mass concentration of adsorbent in the flue gas is  $0.5 \text{ g}/\text{m}^3$  (d.b., s.c.),  $C_0 = 400 \text{ mg}/\text{m}^3$  (d.b., s.c.).

which means that the adsorption is able to take 30% of the mercury out of the flue gas under these conditions.

Fig. 6 shows the influence of the adsorbent capacity on the mercury capture with the adsorbent and on the mercury concentration in the flue gas. The lower diagram gives the changes in the flue gas concentration and the upper diagram in the Hg concentration on the adsorbent. The tendencies are clearly visible: with higher adsorbent capacity the Hg concentration on the adsorbent at the end of the flue gas duct becomes higher. It increases from  $48 \text{ mg Hg}/\text{kg}$  at  $50 \text{ mg}/\text{kg}$  capacity to approximately  $700 \text{ mg Hg}/\text{kg}$  at  $1000 \text{ mg}/\text{kg}$  adsorbent capacity. At the same time the outlet flue gas concentration of mercury is decreasing from  $375 \text{ µg}/\text{m}^3$  (d.b., s.c.) at  $50 \text{ mg}/\text{kg}$  capacity to  $150 \text{ µg}/\text{m}^3$  (d.b., s.c.) at  $1000 \text{ mg}/\text{kg}$  capacity.

Fig. 7 shows the influence of the mass of adsorbent that is injected into the flue gas on the Hg concentration of the flue gas and on the adsorbent. The upper diagram gives the changes in the flue gas concentration and the lower diagram in the Hg concentration on the adsorbent. In this case the mass concentration was varied between  $0.1$  and  $2 \text{ g}/\text{m}^3$  (d.b., s.c.), which refers to  $2.5$  and  $50 \text{ kg}/\text{h}$ , respectively, at the flue gas volumetric flow of  $25,300 \text{ m}^3$  (d.b., s.c.). The Hg concentration of the flue gas decreases from  $380 \text{ µg}/\text{m}^3$  (d.b., s.c.) at  $2.5 \text{ kg adsorbent}/\text{h}$  to  $150 \text{ µg}/\text{m}^3$  (d.b., s.c.) at  $50 \text{ kg adsorbent}/\text{h}$ . The mercury content of the adsorbent decreases with increasing adsorbent injection mass from  $170 \text{ mg}/\text{kg}$  at  $2.5 \text{ kg adsorbent}/\text{h}$  to  $125 \text{ mg}/\text{kg}$  at  $50 \text{ kg}/\text{h}$ .

Fig. 8 presents the relationship between the Hg concentration in the flue gas and on the adsorbent and the specific surface area of the adsorbent. The specific surface area represents both the outer surface area of the particles and the inner surface of the pores. The diagram shows the following tendencies: with an increase of the specific surface area from  $50$  to  $1000 \text{ m}^2/\text{g}$  the flue gas concentration at the end of the flue gas path decreases from  $385$  to  $290 \text{ µg}/\text{m}^3$  (d.b., s.c.). Simultaneously, the concentration on the adsorbent is increasing from  $27 \text{ mg Hg}/\text{kg}$  at  $50 \text{ m}^2/\text{g}$  to  $213 \text{ mg}/\text{kg}$  at  $1000 \text{ m}^2/\text{g}$ .

#### 4.2. Modeling the mercury capture by sorbent injection for the InfraServ case

As a practical example the injection of an adsorbent into the flue gas upstream of the ESP is modeled for the conditions of the InfraServ plant. The operating data and the geometry of the flue gas duct have already been given in Table 5. Since adsorbents based on activated carbon cannot be used at the boiler exit temperature of  $220^\circ\text{C}$  due to the risk of hot spots, the S-zeolite with its characteristics given above is used for the present simulation. The mercury concentration was measured in 1999 at the exit of the boiler to be  $230 \text{ µg}/\text{m}^3$  (d.b., s.c.). This latter value provides the starting condition for the calculation.

In the calculations it was immediately found that the flue gas duct between the boiler and the inlet of the ESP does not provide enough residence time for gas and adsorbent to yield a satisfactory effect. However, the residence time inside the ESP is long and certainly provides space and time for adsorption. As a first approximation the calculation was made with taking 50% of the gas residence time inside the ESP into account (i.e. the simulation assumes that the whole solids capture occurs instantaneously after 50% of the gas residence time in the ESP. Therefore, the calculations in Fig. 9 were made until a total gas residence time of  $3 + 12/2 = 9 \text{ s}$ .

Fig. 9 shows the change in the Hg concentration of the flue gas depending on the mass of adsorbent injected into the flue gas stream. As explained above the Hg concentration of the flue gas decreases with increasing mass concentration of the S-zeolite. After a residence time of  $9 \text{ s}$  the mercury concentration in the flue gas has been reduced to  $221 \text{ µg}/\text{m}^3$  (d.b., s.c.) at a concentration of  $1 \text{ g zeolite}/\text{m}^3$  (d.b., s.c.), whereas a concentration of  $17.5 \text{ µg}/\text{m}^3$  (d.b., s.c.) is reached at a concentration of  $13.5 \text{ g}/\text{m}^3$  (d.b., s.c.). It should be noted here that the injection of adsorbent which leads to a mass concentration of  $13.5 \text{ g}/\text{m}^3$  of flue gas (d.b., s.c.) is able to reduce the Hg concentration in the flue gas to a level which is below the limit of  $30 \text{ µg}/\text{m}^3$  (d.b., s.c.) set by the current German regulation. However, this requires the feeding of  $340 \text{ kg}/\text{h}$  of adsorbent which is unrealistically high. However, since the goal of this technique is to take just part of the load from the mercury capture in the already existing scrubber it is absolutely not necessary to meet the emission limit with this

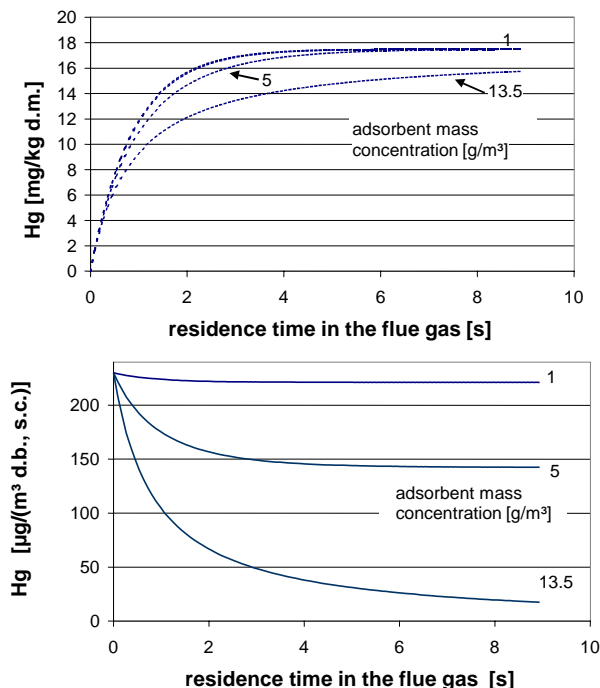


Fig. 9. Comparison of the use of different adsorbent mass concentrations upstream of the electric precipitator of the Höchst plant (for data see Table 5). Simulation of the Hg capture by adsorption as a function of the gas residence time for the conditions of the InfraServ plant (220 °C, S-zeolite).

injection alone. The authors' group is presently investigating sorbents which are especially suited for this application.

#### 4.3. Mercury adsorption on the fly ash

An interesting question is whether the present model is able to simulate the mercury capture by adsorption on the fly ash. It is known that the mercury adsorption on the fly ash depends on the carbon residue in the ash. With increasing content of unburned carbon the adsorption of mercury on the fly ash particle is enhanced [2,4].

A homogeneous distribution of the carbon on fly ash particle surface area is assumed for the modeling. As an additional assumption the ash is removed after half of the residence time in the particle removal device. The calculations are carried out for the Höchst plant. The concentrations of mercury in the flue gas and on the fly ash were measured in 1999. Measurements in the flue gas duct yielded a fly ash loading  $\mu$  in the flue gas of 0.02 kg/kg and Hg concentration in the flue gas at the boiler outlet of 1900  $\mu\text{g}/\text{m}^3$ . Fly ash samples had a specific surface area of 356  $\text{m}^2/\text{kg}$ . The measurement of the adsorption isotherm yielded  $k_{\text{ads}} = 8350 \text{ kg}/(\text{m}^2 \text{ s})$  and  $X_{\text{eq}} = 17.5 \times 10^{-6} \text{ kg}/\text{kg}$ . Fig. 10 shows the comparison of the simulation results and the measured concentrations in the flue gas and on the ash, respectively.

Considering the wide scatter of the measurements (which is not uncommon with this type of measurements) the agreement between measurements and simulation is quite satis-

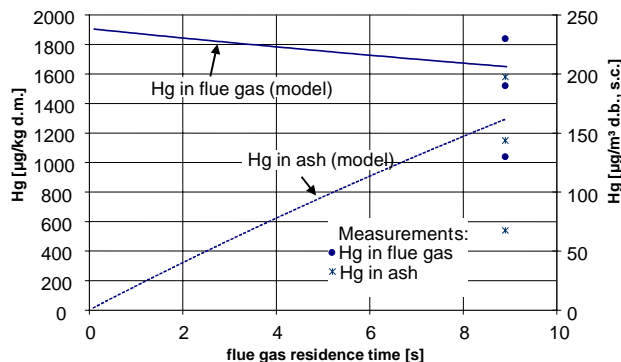


Fig. 10. Comparison of the simulation with measurements of the mercury removal with the fly ash captured in the ESP of the InfraServ plant.

factory. There are two reasons of this scatter. The first one is the fluctuation of the Hg concentration in the flue gas with time which is due to fluctuations of the Hg concentration in the input sludge and the second is the problem of obtaining representative solid samples for Hg analysis from an inhomogeneous material such as fly ash.

## 5. Summary and conclusions

In the present work a model has been suggested which is able to describe the adsorption of mercury by injection of adsorbents into the flue gas path of a waste incinerator.

The necessary adsorption parameters were determined by measuring breakthrough curves in a laboratory-scale fixed bed. The adsorption isotherms for the investigated fly ashes were of the Langmuir type whereas for the investigated activated coals and zeolites they were of the Freundlich type.

The model was applied to simulate the mercury capture in the flue gas path between boiler and ESP and inside the ESP for an existing large-scale sewage sludge incineration plant. Furthermore, the model was used to estimate the mercury capture with the fly ash in the same plant. The agreement between the simulation results and the available measurements was quite satisfactory.

The model can be used in the development of technologies for the adaptation of existing flue gas treatment facilities of incineration plants to more severe requirements for mercury capture.

## References

- [1] H. Czichos, Hütte, Die Grundlagen der Ingenieurwissenschaften, 29th ed., Springer, Berlin, 1991.
- [2] K.C. Galbreath, C.J. Zygarić, Mercury transformations in coal combustion flue gas, Fuel Process. Technol. 65–66 (2000) 289–310.
- [3] W. Gerhartz (Ed.), Ullmanns Encyclopedia of Industrial Chemistry, vol. 3: Unit Operations II, 5th ed., VCH, Weinheim, 1988.
- [4] H. Gutberlet, A. Spiesberger, F. Kastner, J. Tembrink, Zum Verhalten des Spurenelementes Quecksilber in Steinkohlefeuerungen mit Rauchgasreinigungsanlagen, VGB Kraftwerkstechnik, vol. 72, no. 7, 1992, pp. 636–641.



- [5] O. Malerius, J. Werther, M. Mineur, Optimization of mercury capture in a sewage sludge incineration plant, *VGB PowerTech* 4 (2003) 92–98.
- [6] F. Meserole, R. Chang, T. Carey, Modeling mercury removal by sorbent injection, *J. Air Waste Manage. Assoc.* 49 (1999) 694–704.
- [7] S. Serre, G. Silcox, Adsorption of elemental mercury on the residual carbon in coal fly ash, *Ind. Eng. Chem. Res.* 39 (2000) 1723–1730.
- [8] M. Saenger, J. Werther, H. Hanssen, Concentrations and mass balance of mercury in a fluidized bed sewage sludge incineration plant, in: R.B. Reuther (Ed.), *Proceedings of the 15th International Conference on Fluidized Bed Combustion*, ASME, New York, 1999.